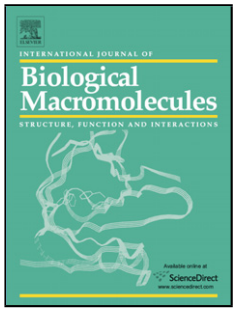

Title: An electrochemical nitric oxide biosensor based on immobilized cytochrome c on a chitosan-gold nanocomposite modified gold electrode

Authors: Ehsan Pashai, Ghasem Najafpour Darzi, Mohsen Jahanshahi, Fatemeh Yazdian, Mostafa Rahimnejad

PII: S0141-8130(17)34245-9
DOI: https://doi.org/10.1016/j.ijbiomac.2017.11.157
Reference: BIOMAC 8637

To appear in: *International Journal of Biological Macromolecules*

Received date: 29-10-2017
Revised date: 25-11-2017
Accepted date: 25-11-2017

Please cite this article as: Ehsan Pashai, Ghasem Najafpour Darzi, Mohsen Jahanshahi, Fatemeh Yazdian, Mostafa Rahimnejad, An electrochemical nitric oxide biosensor based on immobilized cytochrome c on a chitosan-gold nanocomposite modified gold electrode, International Journal of Biological Macromolecules https://doi.org/10.1016/j.ijbiomac.2017.11.157

An electrochemical nitric oxide biosensor based on immobilized cytochrome c on a chitosan-gold nanocomposite modified gold electrode

Ehsan Pashai[a], Ghasem Najafpour Darzi[a,*] Mohsen Jahanshahi[a], Fatemeh Yazdian[b] , Mostafa Rahimnejad[a]

[a] Faculty of Chemical Engineering, Babol Noshirvani University of Technology, Babol, Iran

[b] Faculty of New Science and Technology University of Tehran, Tehran, Iran

[*] Corresponding author:

Tel. / Fax No: +981132334204

Email address: najafpour@nit.ac.ir; najafpour8@yahoo.com

Postal address: Faculty of Chemical Engineering

Babol Noshirvani University of Technology

Babol, Iran

Highlights

- A biosensor based on immobilized Cyt c at the CS-MPA-AuNPs nanocomposite layer was successfully fabricated for nitric oxide detection.
- The electrochemical and electrocatalytic behaviors of the resultant Nafion/Cyt c/CS-MPA-AuNPs /SAMs-Au electrode were investigated by cyclic voltammetry (CV), chronoamperometry and impedance techniques.
- The fabricated biosensor exhibited fast response time, low detection limit and wide linear range with good sensitivity, selectivity and stability.

An electrochemical nitric oxide biosensor based on immobilized cytochrome c on a chitosan-gold nanocomposite modified gold electrode

Abstract

Goldnanoparticle (AuNPs), chitosan (CS), cytochrome c (Cyt c) and Nafion were immobilized on the surface of a gold electrode to form a Nafion/Cyt c/CS-3-Mercaptopropionic acid (MPA)-AuNPs/ cysteamine-MPA (SAMs)-Au electrode. The CS-MPA-AuNPs nanocomposite was characterized by UV-vis spectroscopy. Electrochemical behavior of modified electrode was analyzed by electrochemical impedance spectroscopy (EIS), cyclic voltammetry (CV) and chronoamperometry. Uv-vis results showed that CS-MPA-AuNPs nanocomposite could improve electron transfer between Cyt c and electrode surface and keep the catalytic activity of Cyt c. A pair of well defined and reversible redox peaks could be observed for the modified electrode in a 0.1 M phosphate buffer solution (PBS, pH 7.0). The anodic and cathodic peak potentials of Cyt c/CS-MPA-AuNPs/SAMs-Au electrode were at 0.006 V and −0.043 V (vs. Ag/AgCl), respectively. Particular electrocatalytic activity was shown by Cyt c on CS-MPA-AuNPs layer for nitric oxide (NO) reduction. The relationship between peak current and NO concentration was linear in the range of 1×10^{-7} - 21.5×10^{-7} M with a detection limit of 0.45×10^{-7} M (S/N=3).The sensitivity was 0.199 μA/μM. The obtained results indicating that the newly developed biosensor was quite selective and stable which was used for accurate and exact detection of NO.

Keywords: Au Nanoparticle; Cyclic voltammetry; Cytochrome c; Electron Transfer; Nanocomposite; NO biosensensor

1. Introduction

Nitric oxide (NO) is widely interesting for researchers because of its effects on air pollution and especially biological systems. NO can be released by many mammalian cells to play a number of principal biological roles such as blood pressure regulator and neurotransmitter [1]. The regulation or control of the abnormal NO synthesis affects a number of important biological processes and leads to many diseases. From industrial as well as biochemical and medical perspectives, it is important to quantify NO generated in abnormal and normal tissues, including in vivo or in vitro measurements [2]. Therefore, the determination of NO is an essential requirement for the biological activities of tissues. However, the quantification of NO is difficult, since the free radical NO has automatic chemical reactivity with a half-life of a few seconds (about 6 seconds) [3].

There are several methods [4] for the detection of NO, such as UV–visible spectroscopy, electron spin resonance spectroscopy, chemiluminescence, fluorescence and electrochemical methods. Meanwhile, electrochemical techniques are most used because they are very fast, sensitive, inexpensive, and particularly applicable for in vivo detection [5-8]. Nitric oxide is exchanged in different forms including nitrosonium cation, nitroxyl anion, and NO [9]. Due to this redox behavior, NO can be electrochemically detected through electro-reduction or electro-oxidation. Although, measurements based on electrochemical reduction can prevent the interference of oxidizable substances [10].

Many chemical [5, 11-14] and biological [15-17] modified electrodes have been developed to detect the toxic gases. Among them, several proteins have been used in biosensors as an active catalyst [17-21]. Cytochrome c (Cyt c) as the recognizing element for NO detection has been studied by many researchers [15-17, 20-26]. Cyt c is a water soluble redox heme protein with 12.4 kDa molecular weight comprising only 104 amino acids; which plays a vital role in the living organisms by transferring electrons from Cyt c reductase to Cyt c oxidase [27]. The Cyt c in contact with the electrode surface has a weak electron transfer (ET) that results in weak electrochemical performance, maybe due to its denaturation. Therefore, to avoid these problems, the electrode surface should be modified by some materials. Carboxylic group terminated self-assembled monolayers (SAMs- such as 3-Mercaptopropionic acid (MPA)) can be used for immobilization of Cyt c on gold electrode surfaces, because of electrostatic interactions of this protein with its physiological redox partners [28]. This leads to improved ET, which depends on the SAM length. SAMs bind to gold surface through its thiol group. In the past decade, nanomaterials have widely been used as electrocatalysts in NO sensors, due to their small dimension and good electrocatalytic activity [29-32]. The presence of AuNPs acting as electron relays between Cyt c and the electrode can strongly improved ET. Jensen et al.[28] found that AuNPs served as excellent ET relays; that is mostly due to facilitating the electronic coupling between the protein redox center and the electrode surface.

A variety of polymeric materials have been used to immobilize proteins on electrode surface while maintaining its activity [9, 29, 33-38]. Chitosan (CS), a natural biopolymer type, has distinctive chemical and biological properties due to the existence of amino and hydroxyl groups [39]. CS is considered to be a promising material to modify electrode surface; which is a very good matrix for protein or biomacromolecule immobilization [40] due to its good stability, nontoxicity, high mechanical strength, biocompatibility, excellent film-forming ability and high permeability toward water. These properties make it possible to adsorb AuNPs tightly [29]. Deng et al. [29] fabricated a sensitive and selective NO sensor based on Nafion/ CS -multi-walled carbon nanoubes -AuNPs-glassy carbon electrode. Nafion is highly conductive to cations and has been extensively used as a desired modifier for modification of

electrodes. Nafion with negative charge has a high permeability for NO, whereas it prevents diffusion of anions (such as NO_2^-) to the modified electrode surface [41].

In this paper, cytochrome c was immobilized on CS-MPA-AuNPs/Au electrode and its electrocatalytic activity in NO reduction was investigated. The CS-MPA-AuNPs nanocomposite was characterized by UV-vis spectroscopy. A nafion film was coated on the modified electrode to minimize interferences in detection process. Electrochemical behavior of the resultant Nafion/Cyt c/CS-MPA-AuNPs /SAMs-Au electrode was studied by electrochemical impedance spectroscopy (EIS), cyclic voltammetry (CV) and chronoamperometry techniques. It was found that the modified electrode exhibited prefect electrocatalysis towards NO.

2. Experimental

2.1. Reagents and chemicals

Cytochrome c from bovine heart (5 mg protein/mL), gold chloride trihydrate ($HAuCl_4 \cdot 3H_2O$, ≥ 99.9% trace metals basis), trisodium citrate dehydrate, chitosan (CS, ≥ 75% deacetylation), N-hydroxysuccinimide (NHS, 98%), 1-[3-(Dimethylamino)propyl]-3-ethylcarbodiimide methiodide (EDC methiodide), cysteamine (~95%), potassium ferricyanide ($K_3Fe(CN)_6$, 99%) and Nafion (5wt% solution in a mixture of lower aliphatic alcohols and water) were purchased from Sigma and used as received. The other reagents (such as 3-Mercaptopropionic acid (MPA, ≥ 98%), Pyrogallol (ACS reagent, ≥99%)) were purchased from Merck Company (Darmstadt, Germany). A series of phosphate buffer saline solutions (PBS, 0.1 M, pH 7.4) were prepared by solving 80 g NaCl, 2 g KCl, 14.4 g Na_2HPO_4 and KH_2PO_4 in one liter distillated water and used as supporting electrolyte. All solutions were prepared with double distilled water purified by a Millipore-Q System (18.2 MΩ cm). A Cyt c solution (200 μM) was prepared in 0.1 M PBS (pH 7.0).

2.2. Instrumentation

All electrochemical experiments were carried out with a computer-controlled model VSP electrochemical workstation (BioLogic Science Instruments Co., Paris, France) at room temperature. A conventional three-electrode cell was employed with a Pt counter electrode, an Ag|AgCl reference electrode and a modified gold working electrode. All potentials were represented versus the Ag|AgCl reference. Freshly prepared 10 mL of 0.1 M PBS (pH 7.0) was used as supporting electrolyte. To prepare deoxygenated environment for experiments, the supporting electrolyte was bubbled with highly-purity nitrogen for 30 min and maintained nitrogen condition during the experiments in the glove box. UV-vis

measurements were conducted using a SPEKOL 1500 spectrophotometer (Analytik Jena AG-Germany) with subtraction from blank solutions.

2.3. Preparation of NO standard solutions

NO standard solution was produced according to the literature [2]. This gas was generated by dropwise addition of 2 M H_2SO_4 into a glass flask containing saturated $NaNO_2$ solution. In order to remove oxygen and other nitrogen oxides, the produced gas was continuously passed through a 5% (w/v) pyrogallol solution in the saturated and 10% (w/v) potassium hydroxide solutions, respectively. The whole process was conducted in glove box. Before addition of H_2SO_4, the glove box and all apparatus were meticulously degassed with nitrogen gas for 30 minutes to exclude O_2, since the generated NO could rapidly react with O_2. The saturated NO concentration in the solution was 1.8 mM at 20 ℃. To generate a saturated NO solution, 10 mL deoxygenated PBS (pH 7.0) containing 0.1 M NaCl was bubbled with produced NO gas for 30 minutes and kept under NO atmosphere till use. NO standard solutions were prepared by consecutive dilutions of a saturated NO solution. These prepared solutions were kept in a glass flask with a rubber stopper and light-free curtain with wrapped foils.

2.4. Preparation of AuNPs-CS nanocomposite

In a typical synthesis route, gold nanoparticles (AuNPs) were synthesized with diameters in the range of 12–48 nm through sodium citrate (Merck, 98%) reduction of $HAuCl_4 \cdot 3H_2O$. In brief, 20 mL of 1 mM $HAuCl_4 \cdot 3H_2O$ was brought to a vigorous boiling and stirring; subsequently, 2 mL of 1% trisodium citrate solution was rapidly added to the solution. The solution was boiled for additional 10 min, during this time, the solution changed color from pale yellow to deep red. The solution was allowed to cool down to room temperature while continuously stirring, and then was stored in a refrigerator until further use [42]. The CS-AuNPs nanocomposite was prepared in the following procedure: at first 1.0 wt % CS solution was prepared by dissolving 100 mg CS in 100 mL of 0.1M acetic acid solution. The mixture was heated at about 40-50 ℃, while continuously stirred for 24 h. Then 10 mL of CS solution was dispersed in 10 mL of AuNPs solution and ultrasonicated (ultrasonic agitation). The final concentration of the CS-AuNPs nanocomposite was 0.5 $mg.mL^{-1}$ CS and one-fold decrease of original AuNPs.

2.5. Chemical modification of Cyt c

The chemical modification of bovine heart Cyt c carried out through the reaction of its lysine residues with carboxyl-terminated thiol derivatives MPA via carbodiimide/N-hydroxysuccinimide (EDC/NHS) activation [24]. The purpose of Cyt c reduction was to obtain stable stock solution;

also to activate its amine groups to bind to the carboxyl groups of MPA attached to the AuNPs. Typically, the 0.1M solution of MPA was prepared into PBS (pH 7.0) and an equimolar amount (0.5 mM) of EDC and NHS were added under stirring condition. Then, 20 μL of this solution was mixed with 0.2 mL of 200 μM Cyt c in PBS and let to react while stirring at room temperature. After 2 h, the protein was reduced by adding ascorbic acid (AA) and then reagents excess was removed with a dialysis bag (sigma, 12 KDa MWCO) before recollection into PBS. The final Cyt c concentrations were estimated by absorption measurements and stock solutions were stored at 4℃.

2.6. Fabrication of Nafion/ Cyt c/MPA-AuNPs-CS/SAMs-Au electrode

Gold electrode (GE, 0.75 mm in diameter) was used as working electrode. The electrode was a gold wire around it was covered with a plastic casing. Prior to modification, tip of the electrode was hand ground on a microcloth pads with Al_2O_3 (1 and 0.05 μm) slurry for 60 s and rinsed with distilled water, and finally air dried. Then it was rinsed for 5 min with piranha solution (a 7:3 mixture of concentrated H_2SO_4 and 30% H_2O_2) and distilled water, respectively. The cleaned electrode was ultrasonicated in distilled water and allowed to dry at room temperature. Freshly cleaned gold planar electrodes (0.45 cm^2 active surfaces) were dipped into SAM consisting of cysteamine and MPA prepared from ethanol containing 0.5 mM cysteamine and 0.1 M MPA solution for an incubation period of 15 min, then the electrode was washed with ethanol and distilled water to separate the un-immobilized SAM molecules from the exterior surface of electrode, followed by blow-drying with nitrogen gas. SAMs bind to gold through its thiol group (see Fig. 1, SAMs-Au electrode). The amine group of cystamine was used to bind to the attached carboxylic group of AuNPs. In fact, cystamine is used for strong binding of nanoparticles to the electrode surface. In order to activate the carboxylic groups of the MPA attached to Au electrode, the SAMs-Au electrode was immersed in a 10 mM PBS (pH7.0) containing 20.0 mM EDC for 12 h. Then, the EDC treated modified electrode was washed with buffer solution. In the following step, 5 μL of prepared AuNPs-CS solution was dropped on the SAMs-Au electrode and the modified electrode was kept in room temperature for 4 h. Subsequently, it was rinsed by distilled water. At this step (AuNPs-CS / SAMs-Au electrode), there is a chemical bind between the carboxylic group of MPA and the amine group of CS. Also, another chemical bind exists between the amine group of cysteamine and the carboxylic group of MPA which is attached to AuNPs. The AuNPs-CS coated electrode was incubated in 0.1 M MPA solution for 15 min, followed by washing and drying. Then, the MPA-AuNPs-CS/SAMs-Au electrode was immersed in the modified Cyt c solution at 4℃ for 12 h. According to this procedure, Cyt c was covalently bonded through its amine groups to the carboxylic groups on the MPA-AuNPs-CS layer, forming amide bonds. Furthermore, the free thiol group of MPA

which is attached to Cyt c interacted with AuNPs and also to the amine groups of CS. It is clear that, the technique of protein immobilization was kind of covalently bonds. The Cyt c/MPA-AuNPs-CS/SAMs-Au electrode was coated by 2 µL of in 0.5 wt% Nafion solution (diluted with ethanol) and subsequently dried at 4℃ for 12 h. Finally, the modified Nafion/Cyt c/MPA-AuNPs-CS/SAMs-Au electrode was rinsed by distilled water to remove weakly bound molecules and stored at 4℃ for further use. The procedure for the modified Au electrode construction is shown in Fig. 1.

2.7. Preparation of samples for spectroscopic analysis

A quartz cuvette was cleaned by immersing it in the piranha solution for 30 min. Then, it was washed with distilled water and air dried at room temperature. Finally, the same amount of AuNPs, MPA-AuNPs-Cyt c and CS-MPA-AuNPs-Cyt c were dropped on three quartz cuvettes and kept at 4 ºC for 6 h.

3. Results and discussion

3.1. Spectroscopic analysis

UV–vis absorbance spectroscopy is usually applied to characterize the conformational change of protein and the interaction between protein and other composition [43]. MPA-AuNPs-Cyt c conjugate was prepared by incubating the modified Cyt c solution with MPA-AuNPs solution for 1 h. Use of the same procedure; CS-MPA-AuNPs-Cyt c conjugate was prepared via incubation of the modified Cyt c solution in CS-MPA-AuNPs solution. Fig. 2 shows the UV–vis absorption of the AuNPs, MPA-AuNPs-Cyt c and CS-MPA-AuNPs-Cyt c conjugate.

As Fig. 2 illustrates, the AuNPs have a characteristic LSPR peak at 525 nm. While, the absorption spectra of MPA-AuNPs-Cyt c conjugate exhibits an LSPR peak at 529 nm and a low intensity protein's Soret band at 410 nm. The Soret band arises primarily due to an electron dipole movement. As previously described, introduction of MPA on AuNPs unables strong attachment to the Cyt c and changes its dielectric constant of the adjacent environment [44]. This change in the dielectric constant lead to 4 nm redshift in the LSPR peak for Cyt c-AuNPs conjugate. The CS-MPA-AuNPs-Cyt c has two adsorption bands at 408 and 532 nm. In addition, the presence of CS causes a redshift (about 3 nm) in the LSPR peak due to strong connection of CS with carboxylic group of MPA-AuNPs. Based on special CS properties mentioned above, it can disperse and adsorb AuNPs tightly. Furthermore, CS prevents aggregation (resulting from the attached MPA) of AuNPs that lead to enhancement of LSPR peak (about %5) compared to MPA-AuNPs-Cyt c. Although, there was no significant change in Soret band for CS-MPA-AuNPs-Cyt c conjugate compared to MPA-AuNPs-Cyt c, which indicates that Cyt c in CS-MPA-AuNPs conjugate can retain its activity center of biological catalysis.

3.2. Electrochemical characterization of Nafion/Cyt c/MPA-AuNPs-CS/SAMs-Au electrode

Fig. 3 shows the electrochemical behaviors of the electrode modified with different layers in 0.1 M PBS (pH 7.0) solution at a scan rate of 100 mVs^{-1}. In fact, no redox peak was observed at the bare Au electrode (curve a). The CVs of the Cyt c/MPA/SAMs-Au (curve b) shows a pair of quasi-reversible redox peaks with anodic peak potential at +0.022 V and cathodic peak potential at -0.045 V. The peak potential separation (ΔE_p) is about 67 mV. It indicates that Cyt c is the most desired protein for electron transfer and it can be used as a test system for direct electron transfer of redox proteins [27]. After the adsorption of AuNPs and CS on the Cyt c/MPA/SAMs-Au electrode, the Cyt c/MPA-AuNPs/SAMs-Au electrode (curve c) and the Cyt c/CS-MPA-AuNPs/SAMs-Au electrode (curve d: E_{pa}=0.006 V, E_{pc}=-0.043 V and ΔE_p=37 mV) showed a pair of stronger redox peak and the current has increased as compared to the Cyt c/MPA/SAMs-Au electrode. This findings suggesting that the electron transfer was promoted by the CS-AuNPs nanocomposite. The CVs of the Cyt c/MPA/SAMs-Au electrode (curve b) and Cyt c/MPA-AuNPs/SAMs-Au electrode (curve c) showed smaller redox peak compared to Cyt c/CS-MPA-AuNPs/SAMs-Au electrode (curve d) (see Fig. 3). That might be referred to the transfer coefficient between electron donor and electron acceptor which is closely related to the distance between electron transferring systems [45]. Therefore, the structure of CS-AuNPs nanocomposite could significantly decrease the distance between the redox center of Cyt c and Au electrode surface; which greatly increase the effective surface area of the modified electrode for the immobilization of a larger number of Cyt c and also provide a good conductivity to improve the electron transfer between Cyt c and Au electrode surface. CS-MPA-AuNPs nanocomposite has provided a biocompatible microenvironment to keep Cyt c biological activity which acts as an effective mediator to immobilize a large number of Cyt c on Au electrode and has good conductivity to improve electron transfer between Cyt c and electrode surface.

Impedance changes of electrode surface during modification process can provide good information about conductivity of immobilized layers on electrode by EIS technique. The modified electrodes were tested by EIS in 5 mM N_2-saturated $[Fe(CN)_6]^{3-/4-}$ solution containing 0.1M KCl and the results were showed as Fig. 4. The resistance of charge transfer (R_{ct}) for SAMs-Au electrode (3380 Ω, curve b) was significantly increased compared to bare Au electrode (355 Ω, curve a). After coating of CS-MPA-AuNPs conjugate on SAMs-Au electrode, the R_{ct} was decreased (2110 Ω, curve c). That indicates good conductivity of CS-MPA-AuNPs conjugate. After the Cyt c was coated on the film, the R_{ct} increased to 5160 Ω (curve d). These results indicate that CS-MPA-AuNPs conjugate can enhance the electron transfer due to good conductivity.

3.3. Electrochemical behavior and amperometric response of NO on modified electrode

Fig. 5 shows CVs of the Cyt c/CS-MPA-AuNPs/SAMs-Au electrode in the presence of NO in oxygen-free (N_2-saturated) 0.1 M PBS (pH 7.0) solution. CVs were recorded for the modified electrode by cycling the potential between 0.2 V and -1.0 V (scan rate 100 mVs^{-1}) in absence and presence of nitric oxide (different concentrations). According to Fig. 3, the redox potentials of Cyt c on bare electrodes and modified electrode were about 0 V versus reference electrode. Also the redox peaks were observed in Fig. 5. The reduction peaks for Cyt c-mediated catalytic redox NO were in the range of −0.7 V to -0.8 V [16, 46]. As it turns out, the reaction between Cyt c and NO shifted the reduction potential from 0 to −0.7 V on the Nafion/Cyt c/MPA-AuNPs-CS/SAMs-Au electrode; that has shown Cyt c-mediated NO reduction (see Fig. 5). The reduction peak current has significantly increased; which is showing an electrocatalytic reduction process of NO (curve b and c) as compared to that in the absence of NO (curve a). These results confirmed that the catalytic current of Nafion/Cyt c/MPA-AuNPs-CS/SAMs-Au electrode mainly resulted from the Cyt c electrocatalytic reduction of NO [47]. The CS-MPA-AuNPs nanocomposite layer on the Au electrode might have a catalytic effect in decreasing the reduction potential difference in addition to stabilizing the immobilization of Cyt c on the Au electrode surface. According to the obtained results, amperometric experiments were performed at an applied potential of −0.7 V versus reference electrode.

Fig. 6a displays the typical current-time curves of the Nafion/Cyt c/MPA-AuNPs-CS/SAMs-Au electrode toward the reduction of NO. The amperometric responses of the biosensors were studied by injecting NO solutions into the 0.1 M PBS (pH 7.0) solution under stirring condition. The reduction current steeply rose to reach a maximum steady-state value and achieved 95% of the steady-state current (I_{ss}) within 5 s. Such a fast response can be related to the high electrical conductivity of CS-MPA-AuNPs nanocomposite. Furthermore, this nanocomposite has a good effective surface to immobilize Cyt c and decrease the distance between Cyt c and electrode surface. While the biological activity of the Cyt c was protected by specific biocompatible environment of CS-MPA-AuNPs nanocomposite. Fig. 6b shows the calibration curve of the fabricated NO biosensor. The linear range of the NO detection was from 10 to 215 μM (R=0.999, n=20). The detection limit of this biosensor was estimated to be 4.5 μM and the sensitivity was 0.1995 μA/μM based on the criterion of a signal-to-noise ratio of 3 (S/N=3).

Table 1 showed the characteristics of some reported nitric oxide biosensors. Generally, high performance and accuracy of biosensor are represented by short response time, low detection limit and broad linear range. All these parameters should not necessarily be superior to the corresponding parameters in biosensors; but for any special case of fabricated biosensor, the average of these parameters should be analyzed and evaluated. As can be seen, the prepared biosensor has a lower detection limit, a wider linear range and less response time compared to most of the biosensors stated in Table 1. Therefore,

it can be concluded that the fabricated biosensor performance is much higher than other biosensors. In fact the fabricated biosensor can be effective in online measurement of NO.

3.4. Repeatability, reproducibility, stability and selectivity of the modified electrode

The repeatability of the current response of one resultant modified electrode to five successive amperometric measurements of 1 mM NO was examined. A relative standard deviation value (RSD) of 4.38 % was obtained for the steady current density. The reproducibility of the current response of the same modified electrode was examined in 0.1 M PBS (pH 7.0) containing 1 mM NO by five different modified electrodes. The relative standard deviation was 3.4 % for these assays. The stability of the modified electrode was also studied. When the electrode was stored in N_2-saturarted 0.1 M PBS (pH 7.0) solution at 4 ℃ for two weeks, there was no obvious change of current. At the stated condition, the modified electrode was stored for duration of four weeks. After that, the current response to 1 mM NO only decreased by 3.7 % from the original value. The good stability and reproducibility imply the good biocompatibility of CS-MPA-AuNPs and strong interactions between AuNPs and CS. The role of Nafion in increasing the stability of the electrode should not be ignored.

As noted earlier, Nafion has a high permeability for NO, whereas it prevents diffusion of anions interferences such as NO_2^- and AA to the modified electrode surface. The selectivity of the modified electrode for NO detection was investigated by sequential injections of 15 μM NO, 150 μM NO_2^- and 150 μM AA into the stirring 0.1 M PBS (pH 7.0) as shown in Fig. 7. These interferences had no response during detection of NO. This indicates that the immobilized Nafion on Cyt c/MPA-AuNPs-CS/SAMs-Au electrode has significantly eliminated the interferences of NO_2^- and AA during NO detection. Therefore, it can be concluded that this biosensor had selective detection for NO in the presence of interfering compounds.

4. Conclusion

A biosensor based on immobilized Cyt c at the CS-MPA-AuNPs nanocomposite layer was successfully fabricated for nitric oxide detection. The interferences from NO_2^- and AA were eliminated by Nafion coating. UV–vis absorption spectra showed that Cyt c molecules kept their native structures at the CS-MPA-AuNPs nanocomposite matrix. The electrochemical and electrocatalytic behaviors of the resultant Nafion/Cyt c/CS-MPA-AuNPs /SAMs-Au electrode were investigated. The results showed that CS-MPA-AuNPs nanocomposite created a good biocompatible environment for the Cyt c to keep the biological activity of its molecules and provided a necessary pathway of electron transfer between Cyt c and the surface of Au electrode. The biosensor represented a supreme electrochemical performance in NO

reduction having a fast response time (5 s), in a wide linear range (10-215 μM) with a low detection limit (about 4.5 μM). Furthermore, the developed and fabricated biosensor exhibited good sensitivity, selectivity and stability. This approach may provide a platform for further study on highly sensitive and stable biosensors with natural biopolymer and nanocomposite materials.

Acknowledgments

The authors wish to acknowledge Biotechnology Research Center and Nanotechnology Research Institute, Noshirvani University of Technology, Babol, Iran for their facilities provided to accomplish present research.

Reference

[1] R. Palmer, D. Ashton, S. Moncada, Vascular endothelial cells synthesize nitric oxide from L-arginine, Nature 333(6174) (1998) 664–666.
[2] C. Li, J. Zang, D. Zhan, W. Chen, C. Sun, A. Teo, Y. Chua, V. Lee, S. Moochhala, Electrochemical Detection of Nitric Oxide on a SWCNT/RTIL Composite Gel Microelectrode, Electroanal 18(7) (2006) 713–718.
[3] D. Wink, J. Mitchell, Chemical biology of nitric oxide: insights into regulatory, cytotoxic, and cytoprotective mechanisms of nitric oxide, Free Radical Bio Med 25 (1998) 434–456.
[4] Z. Taha, Nitric oxide measurements in biological samples, Talanta 61(1) (2003) 3–10.
[5] K. Shibuki, An electrochemical microprobe for detecting nitric oxide release in brain tissue, Neurosci Res 9(1) (1990) 69-76.
[6] T. Haruyama, S. Shiino, Y. Yanagida, E. Kobatake, M. Aizawa, Two types of electrochemical nitric oxide (NO) sensing systems with heat-denatured Cyt c and radical scavenger PTIO, Biosens Bioelectron 13(7-8) (1998) 763-769.
[7] C. Fan, X. Chen, G. Li, J. Zhu, D. Zhu, H. Scheer, Direct electrochemical characterization of the interaction between haemoglobin and nitric oxide, Phys Chem Chem Phys 2(19) (2000) 4409-4413.
[8] V. Brovkovych, E. Stolarczyk, J. Oman, P. Tomboulian, T. Malinski, Direct electrochemical measurement of nitric oxide in vascular endothelium, J Pharm Biomed Anal 19(1-2) (1999) 135-143.
[9] A. Abdelwahab, W.A. Koh, H. Noh, Y. Shim, A selective nitric oxide nanocomposite biosensor based on direct electron transfer of microperoxidase: Removal of interferences by co-immobilized enzymes, Biosens Bioelectron 26(3) (2010) 1080–1086.
[10] J. Pang, C. Fan, X. Liu, T. Chen, G. Li, A nitric oxide biosensor based on the multi-assembly of hemoglobin/montmorillonite/polyvinyl alcohol at a pyrolytic graphite electrode, Biosens Bioelectron 19(5) (2003) 441-445.
[11] T. Malinski, Z. Taha, Nitric oxide release from a single cell measured in situ by a porphyrinic-based microsensor, Nature 358(6388) (1992) 676-678.
[12] P. Vallance, S. Patton, K. Bhagat, R. MacAllister, M. Radomski, S. Moncada, T. Malinski, Direct measurement of nitric oxide in human beings, Lancet 345(8968) (1995) 153-154.
[13] F. Bedioui, S. Trevin, J. Devynck, The use of gold electrodes in the electrochemical detection of nitric oxide in aqueous solution, J Electroanal Chem 377(1-2) (1994) 295-298.
[14] A. Vosoughi, F. Yazdian, G. Amoabediny, M. Hakim, Investigating the effect of design parameters on the response time of a highly sensitive microbial hydrogen sulfide biosensor based on oxygen consumption, Biosens Bioelectron 70 (2015) 106-114.
[15] Y.C. Liu, J. Zhao, W.L. Wu, Z.S. Yang, Direct electrochemical behavior of cytochrome c on DNA modified glassy carbon electrode and its application to nitric oxide biosensor, Electrochim Acta 52(14) (2007) 4848–4852.
[16] W. Koh, M. Rahman, E. Choe, D. Lee, Y. Shim, A cytochrome c modified-conducting polymer microelectrode for monitoring in vivo changes in nitric oxide, Biosens Bioelectron 23(9) (2007) 1374–1381.
[17] M. Hulko, I. Hospach, N. Krasteva, G. Nelles, Cytochrome C Biosensor—A Model for Gas Sensing, Sensors 11 (2011) 5968-5980.
[18] B. Ge, F. Lisdat, Superoxide sensor based on cytochrome c immobilized on mixed-thiol SAM with a new calibration method, Anal Chim Acta 454(1) (2002) 53–64.
[19] M. Célia, M. Silveira, A. Gabriela, Small electron-transfer proteins as mediators in enzymatic electrochemical biosensors, Anal Bioanal Chem 405(11) (2013) 3619–3635.

[20] L. Wan, Y. Song, H. Zhu, Y. Wang, L. Wang, Electron Transfer of Co-immobilized Cytochrome c and Horseradish Peroxidase in Chitosan-Graphene Oxide Modified Electrode, Int J Electrochem Sci 6 (2011) 4700 – 4713.
[21] Y. Li, Q. Liu, X. Liang, Q. Xiao, Y. Fang, Y. Wu, A new fluorescence biosensor for nitric oxide detection based on cytochrome P450 55B1, Sensor Actuat B Chem 230 (2016) 405–410.
[22] M. KarimiPur, M. Hosseini, F. Faridbod, A.S. Dezfuli, M. Ganjali, A novel solid-state electrochemiluminescence sensor for detection of cytochrome c based on ceria nanoparticles decorated with reduced graphene oxide nanocomposite, Anal Bioanal Chem 408(25) (2016) 7193–7202.
[23] W. Albery, A. Cass, B. Mangold, Z. Shu, Inhibited Enzyme Electrodes. Part 3: A Sensor for Low Levels of H2S and HCN, Biosens Bioelectron 5(5) (1990) 397-413.
[24] G. Suarez, C. Santschi, O. Martin, V. Slaveykov, Biosensor based on chemically-designed anchorable cytochrome c for the detection of H2O2 released by aquatic cells, Biosens Bioelectron 42 (2013) 385–390.
[25] Y. Song, H. Liu, L. Wan, Y. Wang, H. Hou, L. Wang, Direct Electrochemistry of Cytochrome c Based on Poly(diallyldimethylammonium Chloride)- Graphene Nanosheets/Gold Nanoparticles Hybrid Nanocomposites and Its Biosensing, Electroanal 25(6) (2013) 1400 – 1409.
[26] Y. Hibino, S. Kawai, Y. Kitazumi, O. Shirai, K. Kano, Mutation of heme c axial ligands in D-fructose dehydrogenase for investigation of electron transfer pathways and reduction of overpotential in direct electron transfer-type bioelectrocatalysis, Electrochem commun 67 (2016) 43-46.
[27] C. Mu, Q. Zhao, D. Xu, Q. Zhuang, Y. Shao, Silicon Nanotube Array/Gold Electrode for Direct Electrochemistry of Cytochrome c, J Phys Chem B 111(6) (2007) 1491-1495.
[28] P. Jensen, Q. Chi, F. Grumsen, J. Abad, A. Horsewell, D. Schiffrin, J. Ulstrup, Gold nanoparticle assisted assembly of a heme protein for enhancement of long-range interfacial electron transfer, J Phys Chem C 111(16) (2007) 6124-6132.
[29] X. Deng, F. Wang, Z. Chen, A novel electrochemical sensor based on nano-structured film electrode for monitoring nitric oxide in living tissues, Talanta 82(4) (2010) 1218–1224.
[30] A. Gutierrez, S. Griveau, C. Richard, A. Pailleret, S. Granados, F. Bedioui, Hybrid Materials from Carbon Nanotubes, Nickel Tetrasulfonated Phthalocyanine and Thin Polymer Layers for the Selective Electrochemical Activation of Nitric Oxide in Solution, Electroanalysis 21(21) (2009) 2303-2310.
[31] J. Fei, S. Hu, K. Shiu, Amperometric determination of nitric oxide at a carbon nanotube modified electrode with redox polymer coating, J Solid State Electrochem 15(3) (2011) 519-523.
[32] Q. He, D. Zheng, S. Hu, Development and application of a nano-alumina based nitric oxide sensor, Microchim Acta 164(3-4) (2009) 459–464.
[33] M. Rahman, N. Kwon, M. Won, E. Choe, Y. Shim, Functionalized conducting polymer as an enzyme-immobilizing substrate: an amperometric glutamate microbiosensor for in vivo measurements, Anal Chem 77(15) (2005) 4854-4860.
[34] D. Talarico, F. Arduini, A. Amine, I. Cacciotti, D. Moscone, G. Palleschi, Screen-printed electrode modified with carbon black and chitosan: a novel platform for acetylcholinesterase biosensor development, Anal Bioanal Chem 408(26) (2016) 7299–7309.
[35] C. Kaçar, P.E. Erden, E. Kılıc, Amperometric L-lysine enzyme electrodes based on carbon nanotube/redox polymer and graphene/carbon nanotube/redox polymer composites, Anal Bioanal Chem 409(11) (2017) 2873–2883.
[36] Y. Wang, S. Hu, Nitric oxide sensor based on poly (p-phenylenevinylene) derivative modified electrode and its application in rat heart, Bioelectrochemistry 74(2) (2009) 301-305.
[37] X. Chen, H.Y. Long, W.L. Wu, Z.S. Yang, Direct electrochemical behavior of cytochrome c on sodium dodecyl sulfate modified electrode and its application to nitric oxide biosensor, Thin Solid Films 517(8) (2009) 2787–2791.

[38] A. Ciszewski, G. Milczarek, Electrochemical detection of nitric oxide using polymer modified electrodes, Talanta 61 (2003) 11-26.
[39] Y. Deng, D. Liu, G. Du, X. Li, J. Chen, Preparation and characterization of hyaluronan/chitosan scaffold crosslinked by 1-ethyl-3-(3-dimethylaminopropyl) carbodiimide, Polym Int 56(6) (2007) 738-745.
[40] I.D. Oliveira, I. Vieira, Immobilization procedures for the development of a biosensor for determination of hydroquinone using chitosan and gilo (Solanum gilo), Enzyme Microb Technol 38(3-4) (2006) 449-456.
[41] G. Gerhardt, A. Oke, G. Nagy, Nafion-coated electrodes with high selectivity for CNS electrochemistry, Brain Res 290(2) (1984) 390–395.
[42] M. Omidi, G. Amoabediny, F. Yazdian, M. Habibi-Rezaei, Hydrogen sulfide detection using a gold nanoparticle/metalloprotein based probe, Chin Phys Lett 31(8) (2014) 088701.
[43] C. Guo, Y. Song, H. Wei, P. Li, L. Wang, L. Sun, Y. Sun, Z. Li, Room temperature ionic liquid doped DNA network immobilized horseradish peroxidase biosensor for amperometric determination of hydrogen peroxide, Anal Bioanal Chem 389(2) (2007) 527–532.
[44] M. Omidi, G. Amoabediny, F. Yazdian, M. Habibi-Rezaei, Protein based localized surface plasmon resonance gas sensing, Chin Phys Lett 32(1) (2015) 018701.
[45] J. Xu, F. Shang, J. Luong, K. Razeeb, J. Glennon, Direct electrochemistry of horseradish peroxidase immobilized on a monolayer modified nanowire array electrode, Biosens Bioelectron 25(6) (2010) 1313–1318.
[46] Q. Lu, S. Hu, D. Pang, Z. He, Direct electrochemistry and electrocatalysis with hemoglobin in water-soluble quantum dots film on glassy carbon electrode, Chem Commun (20) (2005) 2584–2586.
[47] M. Zheng, Y. Cui, X. Li, S. Liu, Z. Tang, Photoelectrochemical sensing of glucose based on quantum dot and enzyme nanocomposites, J Electroanal Chem 656(1-2) (2011) 167-173.
[48] Y. Xu, C. Hu, S. Hu, A reagentless nitric oxide biosensor based on the direct electrochemistry of hemoglobin adsorbed on the gold colloids modified carbon paste electrode, Sensor Actuat B Chem 148(1) (2010) 253–258.
[49] W. Wen, W. Chen, Q.Q. Ren, X.Y. Hu, H.Y. Xiong, X.H. Zhang, S.F. Wang, Y.D. Zhao, A highly sensitive nitric oxide biosensor based on hemoglobin–chitosan/graphene–hexadecyltrimethylammonium bromide nanomatrix, Sensor Actuat B Chem 166-167 (2012) 444–450.
[50] Y. Wang, S. Hu, A novel nitric oxide biosensor based on electropolymerization poly(toluidine blue) film electrode and its application to nitric oxide released in liver homogenate, Biosens Bioelectron 22(1) (2006) 10-17.
[51] A. Ananthi, K.L. Phani, Self-assembly of gold nanoparticles on sulphide functionalized polydopamine in application to electrocatalytic oxidation of nitric oxide, J Electroanal Chem 764 (2016) 7-14.

Figure Captions

Fig. 1. Schematic representation of the fabrication of Nafion/ Cyt c/CS-MPA-AuNPs /SAMs-Au electrode

Fig. 2. UV- vis spectra of native AuNPs, Cyt c- MPA -AuNPs and Cyt c-CS- MPA –AuNPs

Fig. 3. CVs of : bare Au electrode (a), Cyt c/MPA/SAMs-Au electrode (b), Cyt c/MPA-AuNPs/SAMs-Au electrode (c) and Cyt c/CS-MPA-AuNPs/SAMs-Au electrode (d) in 0.1 M PBS (pH 7.0) at the scan rate of 100 mVs^{-1}

Fig. 4. Impendence plots of bare Au electrode (a), MPA/Au electrode (b), CS-MPA-AuNPs/Au electrode (c) and Cyt c/CS-MPA-AuNPs/Au electrode in 5 mM $[Fe(CN)_6]^{3-/4-}$ with 0.1 M KCl

Fig. 5. CVs of the Nafion/Cyt c/MPA-AuNPs-CS/SAMs-Au electrode in 0.1 M PBS (pH 7.0) in varying NO concentrations 0 μM (a), 12.5 μM (b) and 50 μM (c) at the scan rate of 100 mVs^{-1}

Fig. 6. (A) Amperometric response of the Nafion/Cyt c/MPA-AuNPs-CS/SAMs-Au electrode to successive injection of NO into 10 mL of stirring 0.1 M PBS (pH 7.0) at an applied potential of -0.7 V (vs. Ag/AgCl). (B) Calibration curve of current to NO concentration. Applied potential −0.7 V (vs. Ag/AgCl), supporting electrolyte 0.1 M PBS (pH 7.0)

Fig. 7. Amperometric response recorded by the Nafion/Cyt c/MPA-AuNPs-CS/SAMs-Au electrode in a 0.1 M PBS (pH 7.0) at an applied potential of -0.7 V (vs. Ag/AgCl) to which 15 μM NO, 150 μM AA, 150 μM NO_2^- and 15 μM NO were added, respectively

Figures :

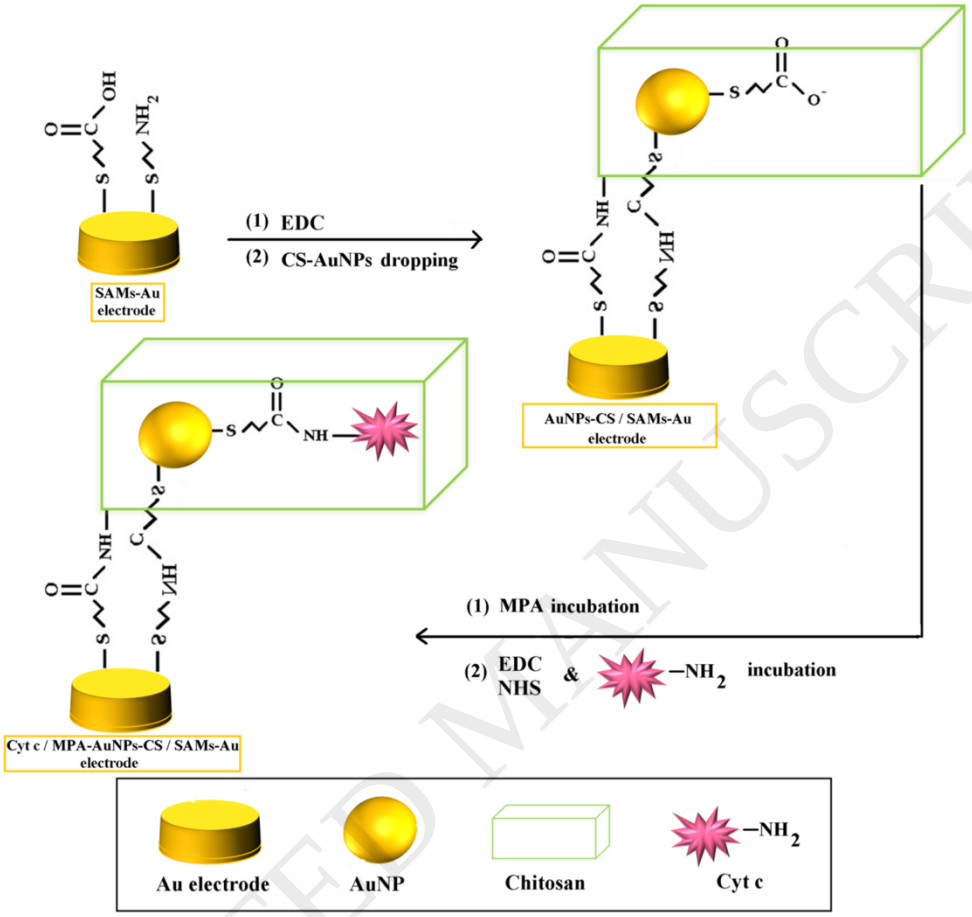

Fig. 1

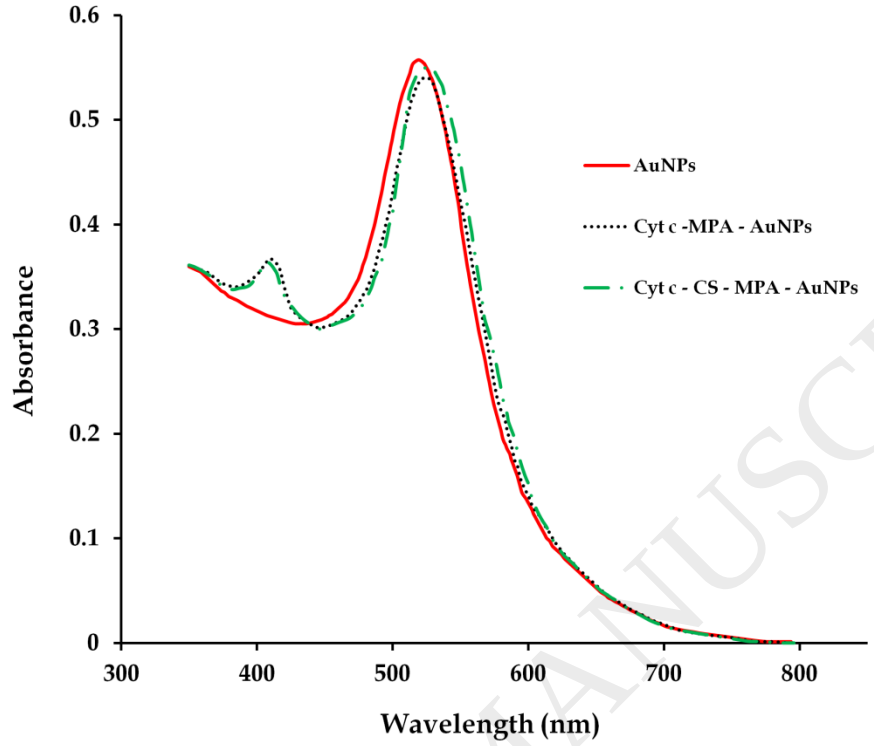

Fig. 2

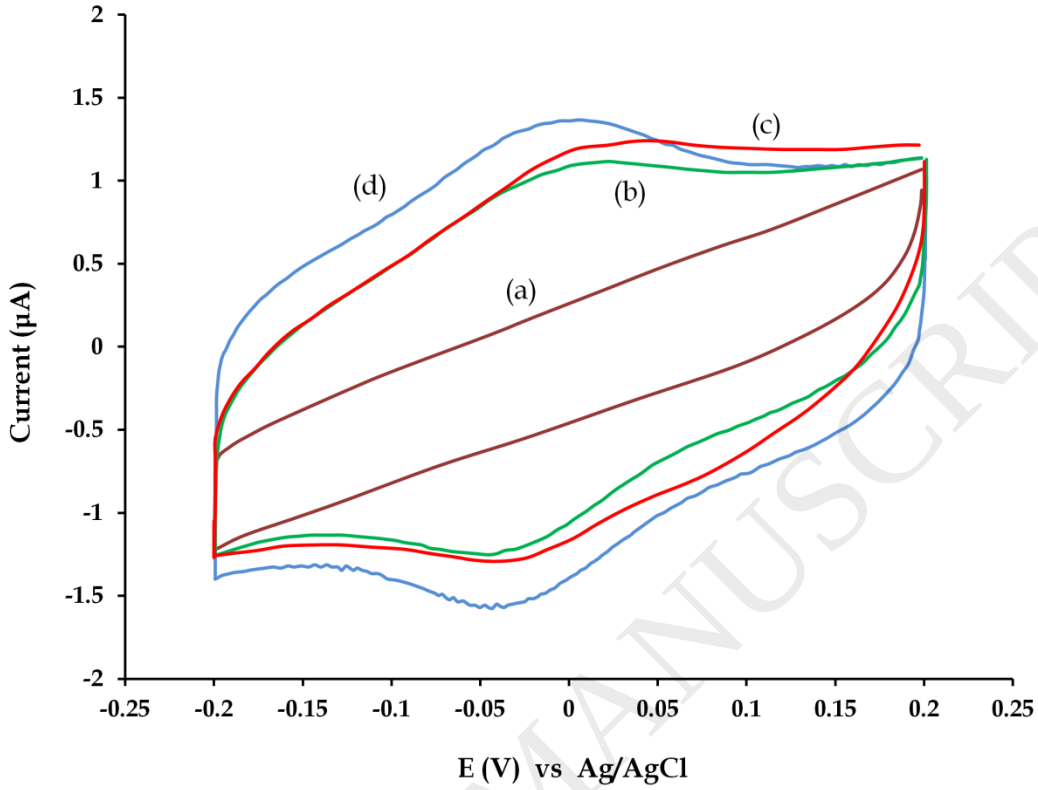

Fig. 3

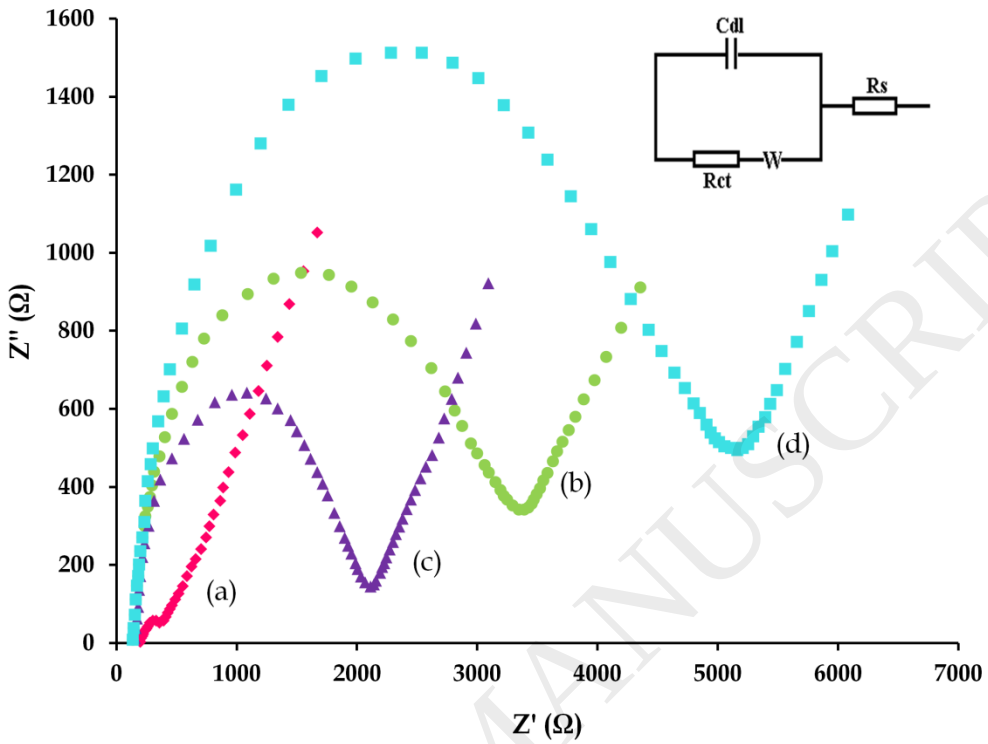

Fig. 4

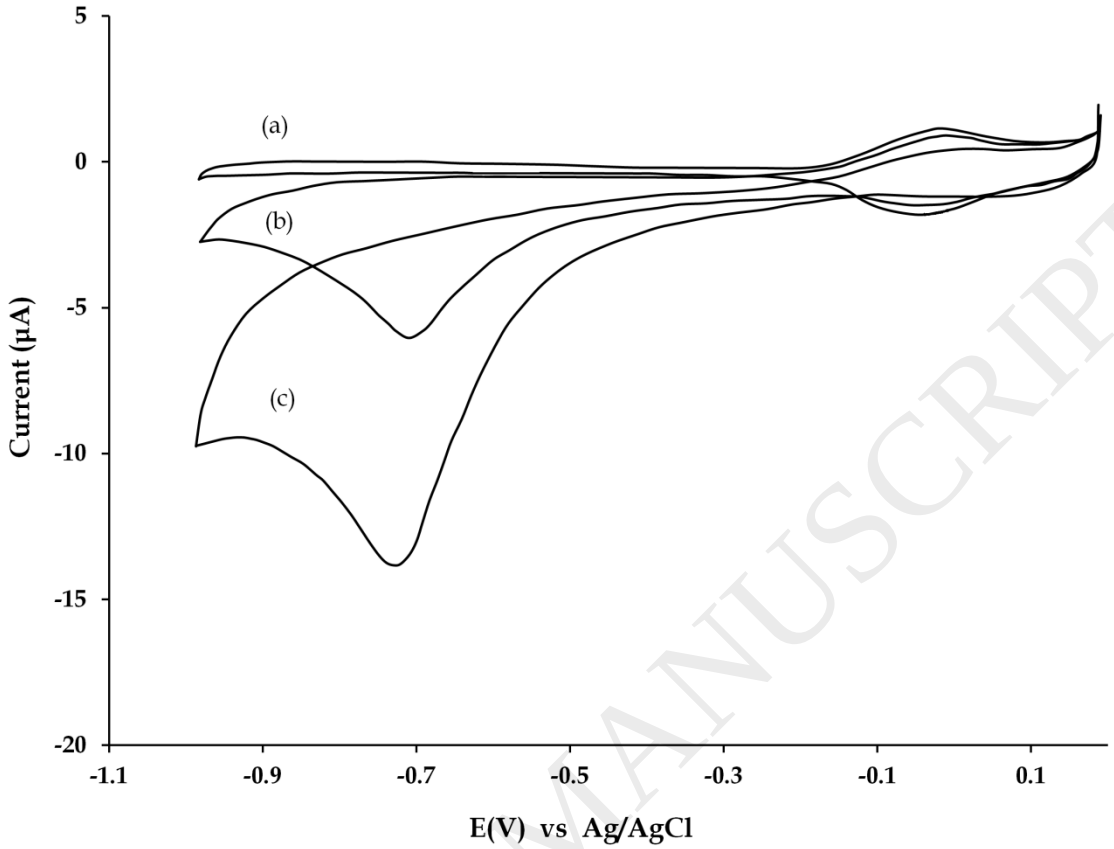

Fig. 5

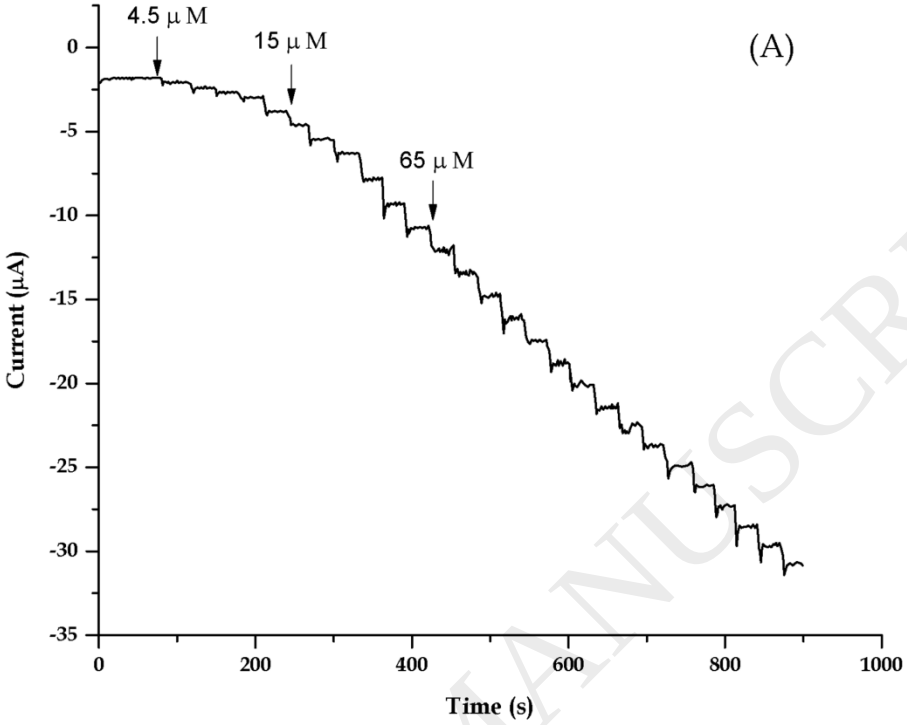

Fig. 6a

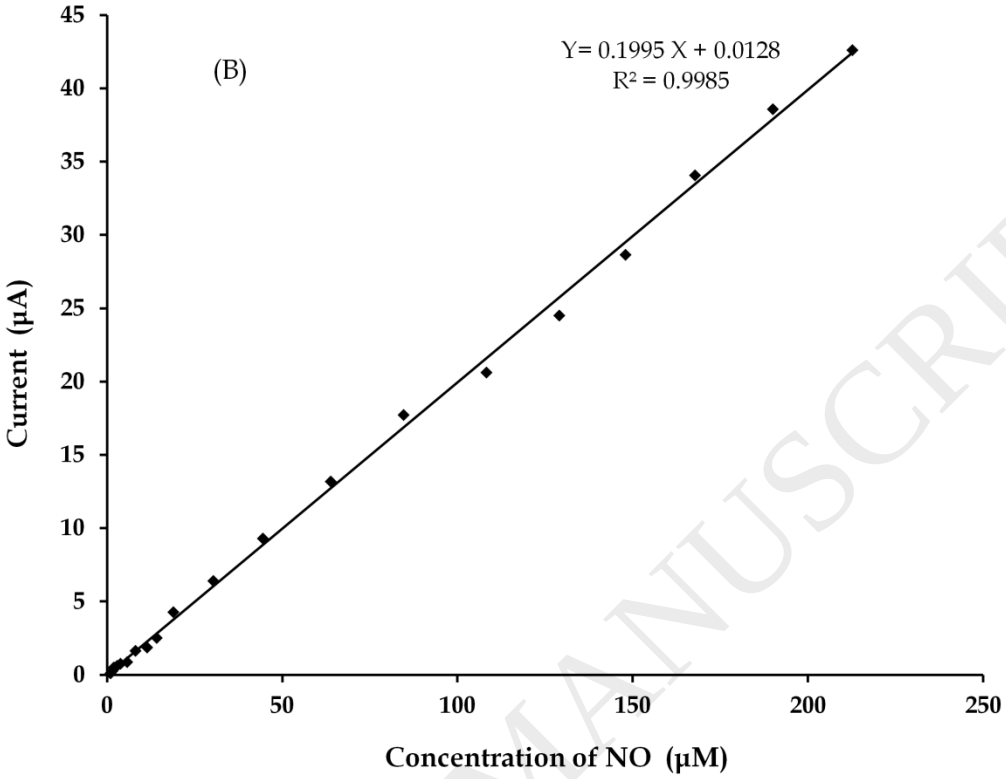

Fig. 6b

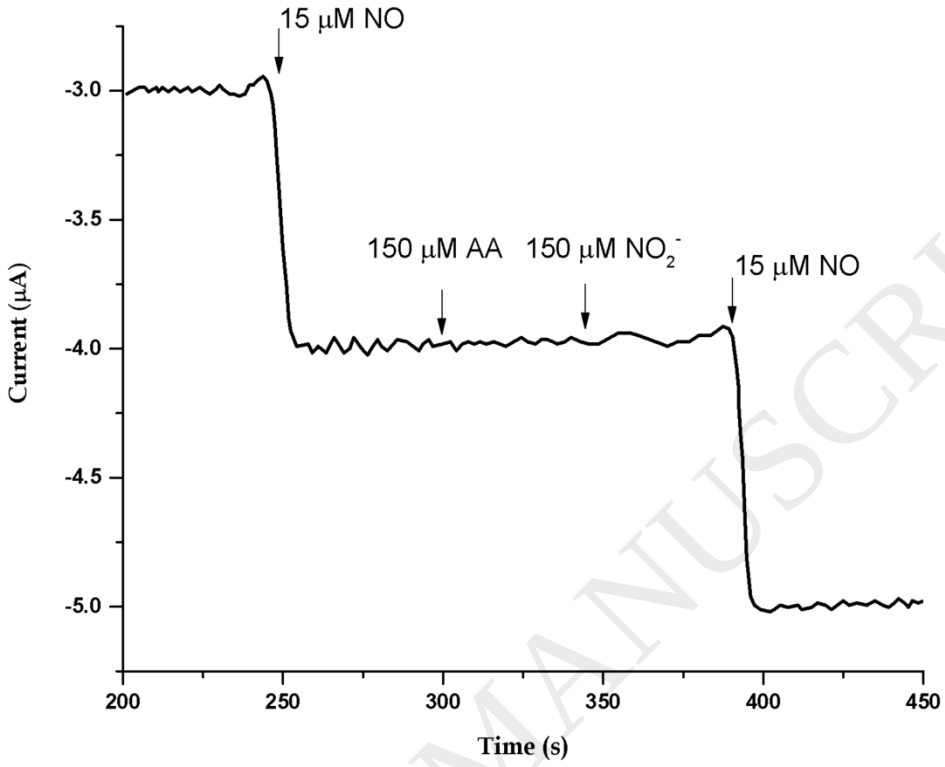

Fig. 7

Tables

Table 1
Comparison of some electrochemical nitric oxide biosensors.

Working electrode	Linear range (M)	Detection limit (M)	Response time (s)	reference
Nafion/cyt c/poly-TTCA/Pt	2.4×10^{-6} - 5.5×10^{-5}	13×10^{-9}	15	[16]
Nafion/MWNTs-CS-AuNPS/GCE	1.9×10^{-7} - 5.4×10^{-5}	76×10^{-9}	4	[29]
PPV derivative/GCE	1.8×10^{-7} - 1.0×10^{-4}	23×10^{-9}	-	[36]
Hb/Au-CPE	9.0×10^{-7} - 3.0×10^{-4}	1×10^{-7}	-	[48]
Hb–CS/GR–CTAB/GCE	2.25×10^{-8} - 2.64×10^{-6}	6.75×10^{-9}	5	[49]
Cyt c/SDS/PAM/GCE	8.0×10^{-7} - 9.5×10^{-5}	1×10^{-7}	< 2	[37]
Hb/MMT/PVA/PG	1.0×10^{-6} - 2.5×10^{-4}	5×10^{-7}	-	[10]
Nafion/PTB/GCE	1.8×10^{-7} - 8.6×10^{-5}	1.8×10^{-8}	-	[50]
Cytochrome c/DNA/GCE	6.0×10^{-7} - 8.0×10^{-6}	1×10^{-7}	-	[15]
AuNPs/S-PDA/GCE	5.0×10^{-6} - 5.5×10^{-5}	25.6×10^{-7}	-	[51]
Cyt c/CS-MPA-AuNPs/SAMs-Au	1.0×10^{-5}-2.15×10^{-4}	45×10^{-9}	5	This work